PROCEEDINGS OF SCIENCE

W and Z Physics at Hadron Colliders

Juan Alcaraz Maestre[*†]
CIEMAT, Centro de Investigaciones Energéticas, Medioambientales y Tecnológicas,
Avda. Complutense 22, 28040 - Madrid, Spain
E-mail: Juan.Alcaraz@cern.ch

We discuss recent results on W and Z physics at LHC and Tevatron colliders. The overview includes W and Z inclusive measurements, differential cross sections and asymmetries at the LHC, as well as new studies on weak boson production in association with heavy quark jets. The single-boson analyses that are described correspond in many cases to final LHC results on 2010 pp collision data at $\sqrt{s} = 7$ TeV, for an integrated luminosity of $\mathscr{L} \approx 35$ pb^{-1}. We also discuss recent results on diboson production and anomalous triple gauge coupling searches, corresponding to the analysis of $\mathscr{L} \approx 6$ fb^{-1} of Tevatron data and ≈ 1 fb^{-1} of LHC data per experiment. The reported results are found to be consistent with Standard Model expectations.

The 2011 Europhysics Conference on High Energy Physics-HEP 2011,
July 21-27, 2011
Grenoble, Rhône-Alpes France

[*]Speaker.
[†]Partially supported by MICINN grant PR2010-0486

PoS(EPS-HEP2011)006

1. Introduction

$W \to \ell\nu$ and $Z \to \ell^+\ell^-$ are among the cleanest final states that can be studied at hadron colliders. They are important channels to understand and calibrate the detector response to leptons: triggering algorithms, identification capabilities, momentum resolution, estimate of efficiencies. W and Z bosons are also part of the dominant signal or background components in many analyses, like top physics, Higgs, SUSY or more exotic searches. The theoretical understanding of weak boson production has improved significantly over the last years and many accurate tools are now at our disposal. Besides the classical generator approaches based on PYTHIA or HERWIG [1], which are kinematically quite precise for final states with weak bosons plus up to one hard jet, there are now dedicated approaches at next order in α_S (NLO), like MC@NLO and POWHEG [2], providing accurate estimates of the total yields at NLO too. Higher order (NNLO) theoretical predictions are available to estimate yields for almost any given set of phase space cuts (FEWZ and DYNNLO [3]) and multiple jet production is reliably simulated at leading order using MLM or CKKW approaches [4]. And there are more improvements to come, like the inclusion of higher order QCD-EWK combined effects or the development of generators for multiple associated jet production accurate at NLO [5].

The following sections summarize just a fraction of the results presented at this Conference. We consider LHC studies of weak boson production, production in association with heavy quark jets, diboson and triple gauge coupling studies. Due to unfortunate limitations of space, we focus only on analyses finalized in the last year, and particularly on new results from the LHC experiments [6]. For other relevant studies developed in the last months, like generic boson plus jet production, $W+2$ jet anomalies or past electroweak measurements by Tevatron experiments [7], we refer to other parallel and plenary presentations at this Conference.

2. Inclusive W and Z cross sections at the LHC

W and Z production at LHC can be visualized at the hard scattering level and at the lowest order as the collision of a valence quark (u or d) and a sea antiquark at the weak boson mass scale ($Q \approx 100$ GeV). Besides this difference - at Tevatron quarks and antiquarks are predominantly valence quarks - the larger center-of-mass energy of the LHC implies typically lower parton fractions of the proton energy, x, in the interval $10^{-3} < x < 10^{-1}$, for central collisions like those recorded by ATLAS and CMS detectors. LHCb has access to larger rapidities and therefore to lower fractions, $10^{-4} < x < 10^{-3}$. At these low values, valence quark production is no longer dominant, and any sensible description of the process involves a significant contribution of sea-sea quark-antiquark interactions. W and Z cross sections at the LHC are expected to be about three times larger than those measured at the Tevatron. For an integrated luminosity of $\mathscr{L} \gtrsim 1$ fb^{-1} one expects millions of $W \to \ell\nu$ and $Z \to \ell^+\ell^-$ per experiment and per lepton channel.

Selecting $W \to \ell\nu$ and $Z \to \ell^+\ell^-$ events is relatively straightforward. Both ATLAS and CMS experiments obtain a high purity $Z \to \ell^+\ell^-$ sample by demanding the presence of two isolated leptons of high transverse momenta, $p_T > 20-25$ GeV, with a reconstructed invariant mass consistent with the Z mass. The excellent detector resolution allows a precise reconstruction of leptonic invariant masses, as illustrated in Fig. 1-left for the case of electron pairs in the central region of

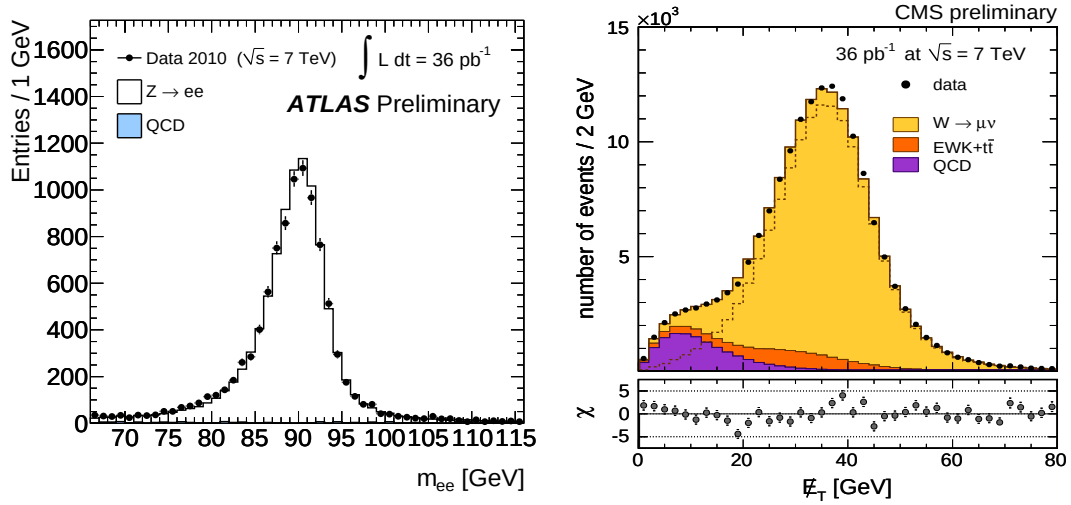

Figure 1: Left: invariant mass of pairs of electrons reconstructed in the central region of the ATLAS detector. Right: $E_{\mathrm{T}}^{\mathrm{miss}}$ distribution of selected $\mathrm{W} \to \mu\nu$ candidates in CMS.

the ATLAS detector. Experiments choose slightly different phase space definitions for the measurement of a total resonant cross section that minimizes the contributions from photon-exchange diagrams (ATLAS: $66 < M_{\ell^+\ell^-} < 116$ GeV, CMS: $60 < M_{\ell^+\ell^-} < 120$ GeV).

The selection criteria for $\mathrm{W} \to \ell\nu$ are chosen to be simple and minimally dependent on details of the missing transverse energy ($E_{\mathrm{T}}^{\mathrm{miss}}$) detector response. Events with one high-p_{T} lepton, $p_{\mathrm{T}} > 20-25$ GeV, well isolated from any tracker or calorimetric activity are considered. A veto on Drell-Yan dileptons is also applied. Fig. 1-right shows the CMS $E_{\mathrm{T}}^{\mathrm{miss}}$ distribution in the muon channel after cuts. The level of background is already low at this stage, even if no $E_{\mathrm{T}}^{\mathrm{miss}}$ cuts are applied. It amounts to a few percent of the total in the signal dominated region $E_{\mathrm{T}}^{\mathrm{miss}} \gtrsim 20$ GeV, where Drell-Yan and $\mathrm{W} \to \tau\nu$ contributions become important. In the CMS case cross sections are determined from fits to the different components of the $E_{\mathrm{T}}^{\mathrm{miss}}$ distribution itself, without further cuts. The most difficult part of the analysis is the estimate of lepton efficiencies and of $E_{\mathrm{T}}^{\mathrm{miss}}$ template shapes for signal and backgrounds, which are extracted from control samples in data. Both experiments determine lepton efficiencies on high-purity $\mathrm{Z} \to \ell^+\ell^-$ samples. One lepton satisfying tight selection criteria is used to tag the presence of a $\mathrm{Z} \to \ell^+\ell^-$ event with high confidence. The second lepton is then used as a probe to determine trigger, isolation, reconstruction and identification efficiencies as a function of p_{T} and pseudorapidity (η).

ATLAS and CMS present at this Conference final results on inclusive W and Z measurements for the integrated luminosity analyzed in 2010, $\mathscr{L} \approx 36$ pb^{-1}. Thanks to the extensive use of data-driven methods for the determination of efficiencies and the description of signals and backgrounds, the uncertainties, summarized in Table 1 have been significantly reduced with respect to previous results at lower luminosities. We draw the attention to the fact that measurements are already dominated by systematic uncertainties. If we ignore the luminosity contribution to the uncertainty, total cross section measurements have comparable theoretical and experimental uncertainties. This is why both collaborations also provide cross section measurements in the fiducial volumes of their

CMS uncertainties (%)	$W \to e\nu$	$W \to \mu\nu$	$Z \to e^+e^-$	$Z \to \mu^+\mu^-$
Statistical	0.3	0.3	1.0	0.8
Experimental (excl. luminosity)	1.5	1.1	1.8	0.7
Luminosity	4	4	4	4
Theory	0.9	1.1	1.7	2.0
Total	4.4	4.3	4.8	4.6

ATLAS uncertainties (%)	$W \to e\nu$	$W \to \mu\nu$	$Z \to e^+e^-$	$Z \to \mu^+\mu^-$
Statistical	0.3	0.3	0.9	0.9
Experimental (excl. luminosity)	2.8	2.4	3.2	1.1
Luminosity	3.4	3.4	3.4	3.4
Theory	3.0	3.0	4.0	4.0
Total	5.3	5.1	6.2	5.4

Table 1: Breakdown of statistical, experimental and theoretical uncertainties in the measurement of total W and Z cross sections by CMS and ATLAS experiments.

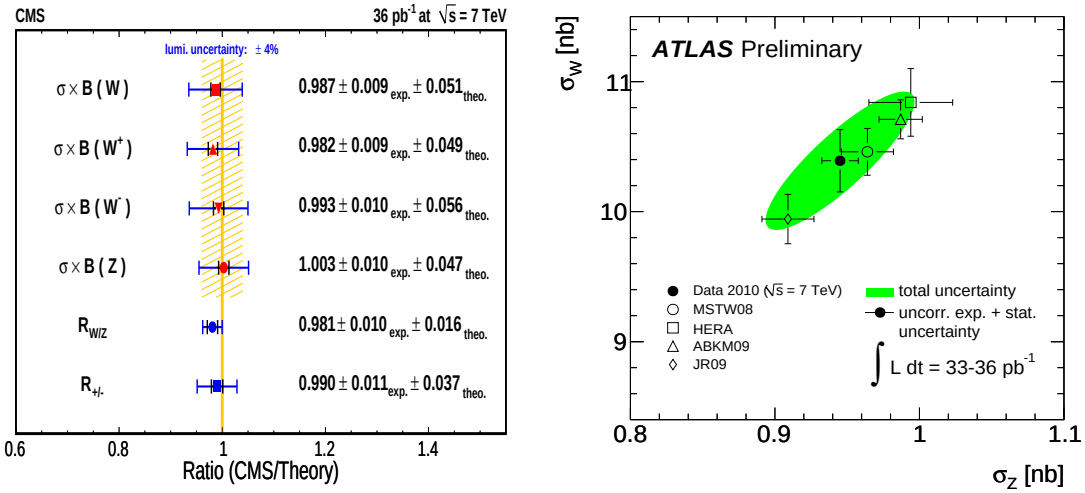

Figure 2: Left: CMS W and Z inclusive measurements compared with theoretical expectations. Measurements of the W/Z and W^+/W^- cross section ratios are also shown. Right: ATLAS measurements of W and Z total cross sections compared with theory predictions for different choices of the parton density functions.

detectors, which are minimally affected by theoretical uncertainties due to acceptance corrections. More details are provided in the corresponding references of ATLAS [8] and CMS [9]. Measurements combining electron and muon channels are graphically shown in Fig. 2. They are found to be in good agreement with theoretical expectations at NNLO.

ATLAS has finalized the 2010 studies on $Z \to \tau^+\tau^-$ production [10] using $\tau_\mu\tau_h$, $\tau_e\tau_h$, $\tau_\mu\tau_e$ and $\tau_\mu\tau_\mu$ final states, where τ_ℓ denotes a tau decay into a charged lepton plus neutrinos and τ_h identifies a tau decay into hadrons plus a tau neutrino. Both ATLAS and CMS have shown remark-

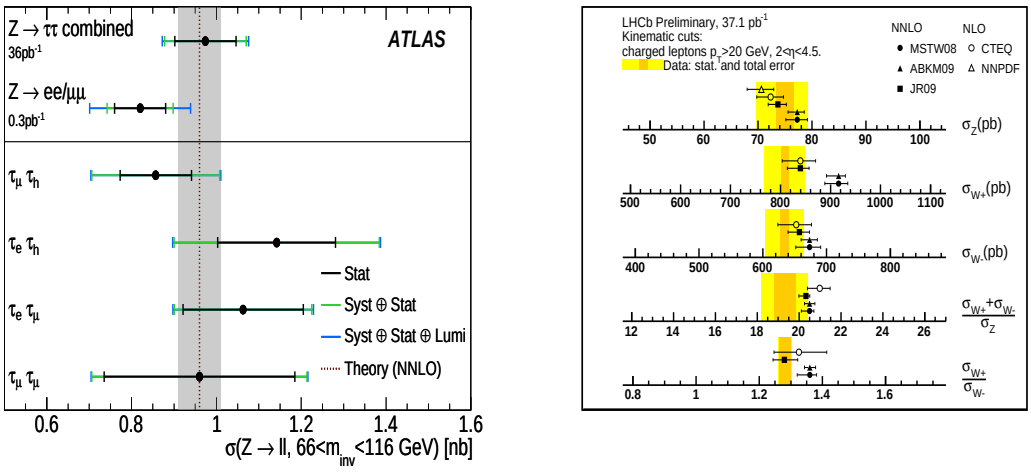

Figure 3: Left: summary of ATLAS measurements of the $Z \to \tau^+\tau^-$ cross section, compared with the equivalent measurement in the electron and muon channels. Right: summary of W and Z results from the LHCb collaboration.

able tau identification capabilities, allowing a clean extraction of $Z \to \tau^+\tau^-$ signals with rather low integrated luminosities. The precise ATLAS measurements of the $Z \to \tau^+\tau^-$ cross section, summarized in Fig. 3-left are consistent with those obtained using electron and muon channels and with corresponding previous measurements of CMS [11]. These impressive results are also good news for future new physics searches involving taus in the final state.

Finally, LHCb has updated previous analyses of W and Z production at high rapidities [12]. These are important measurements because they are sensitive to parton density functions (PDF) of the proton in regions where valence quarks are dominant ($x > 0.1$) as well as to minimally explored regions ($x < 10^{-3}$). While $Z \to \mu^+\mu^-$ decays are cleanly identified thanks to the excellent tracking performance, $W \to \mu\nu$ decays can not be identified via $E_{\mathrm{T}}^{\mathrm{miss}}$, given the specific forward configuration of the experiment. Nevertheless, the presence of an isolated muon with large transverse momentum, $p_{\mathrm{T}\mu} > 20$ GeV, consistent with the primary vertex of the collision is enough to obtain an enriched sample of $W \to \mu\nu$ events. Background components show distinct behaviors as a function of $p_{\mathrm{T}\mu}$ that can be studied on control samples. A summary of the results is shown in Fig. 3-right.

3. Cross section ratios and differential distributions at LHC

The W and Z inclusive cross section results presented in the previous section are affected by large luminosity uncertainties ($> 3\%$). Measurements of cross section ratios are more precise because they are minimally affected by theoretical or experimental biases. This is visible in the W/Z and W^+/W^- ratios measured by CMS and shown in Fig. 2-left, $R_{W/Z}$ and $R_{+/-}$. The equivalent $R_{W/Z}$ measurement from ATLAS corresponds to the central value of Fig. 2-right, with an uncertainty given by half the length of the minor axis of the uncertainty ellipse. One thing to note is that the theoretical uncertainty on $R_{W/Z}$ is small, so the experimental measurement can be interpreted

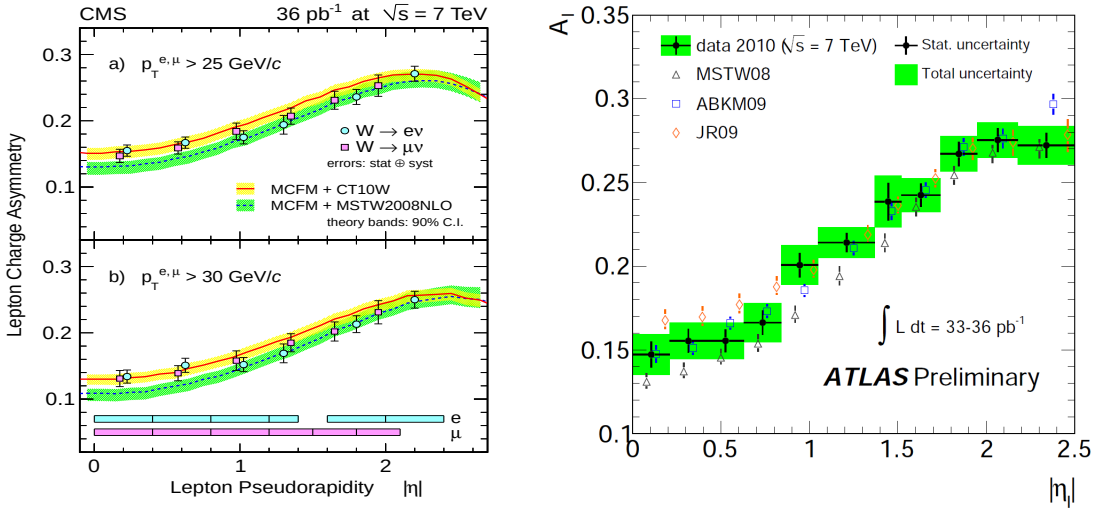

Figure 4: W lepton charge asymmetry measurements of CMS and ATLAS.

as a stringent test of Standard Model predictions. On the contrary, $R_{+/-}$ is dominated by PDF uncertainties that are larger than the experimental ones. Therefore $R_{+/-}$ is a powerful observable to constrain PDFs.

In order to enhance the sensitivity on PDFs, $R_{+/-}$ can be measured in bins of some of the relevant phase space variables, like the charged lepton pseudo-rapidity, $|\eta_\ell|$, or its transverse momentum $p_{\mathrm{T}\ell}$. In practice, experiments measure the W lepton charge asymmetry as a function of $|\eta_\ell|$, $A_l(|\eta_\ell|) \equiv (R_{+/-}(|\eta_\ell|) - 1)/(R_{+/-}(|\eta_\ell|) + 1)$, using analyses similar to the inclusive ones presented before. Results, unfolded to the generator level for an easier comparison with theory are reported in [13, 14] and summarized in Fig. 4. In the case of CMS two different $p_{\mathrm{T}\ell}$ cuts are used, to further exploit the dependences of the asymmetry on $p_{\mathrm{T}\ell}$. Both experiments are consistent with PDF predictions at each measured point within uncertainties, but the shapes as a function of $|\eta_\ell|$ show a tendency that is not reproduced well by most PDF sets. Indeed these measurements are being used already to improve PDF predictions in the relevant region of sensitivity [15]. Last but not least, LHCb measurements at high rapidities have a complementary role to play in these studies, as illustrated in Fig. 5-left [16].

ATLAS has presented at this conference comprehensive comparisons of W and Z differential distributions with theoretical expectations using different NNLO PDF sets [14]. Fig. 5-right shows the case of the Z differential cross section distribution as a function of rapidity, in reasonable agreement with theory. Previous results from CMS on this distribution are reported in Ref. [17].

The CMS collaboration has shown at this conference a final measurement of the dilepton differential cross section distribution as a function of invariant mass [18]. Outside the Z resonance region, the distribution is interesting because it is sensitive to PDF assumptions, it is affected by sizable electroweak corrections and can be potentially modified by new physics effects. Fig. 6-left shows the distribution, unfolded for resolution and final state radiation effects, acceptance corrected and normalized to the to the yield in the resonant region. A full NNLO approach is essential in the analysis, since a substantial fraction of the selected events in the very low invariant mass bins

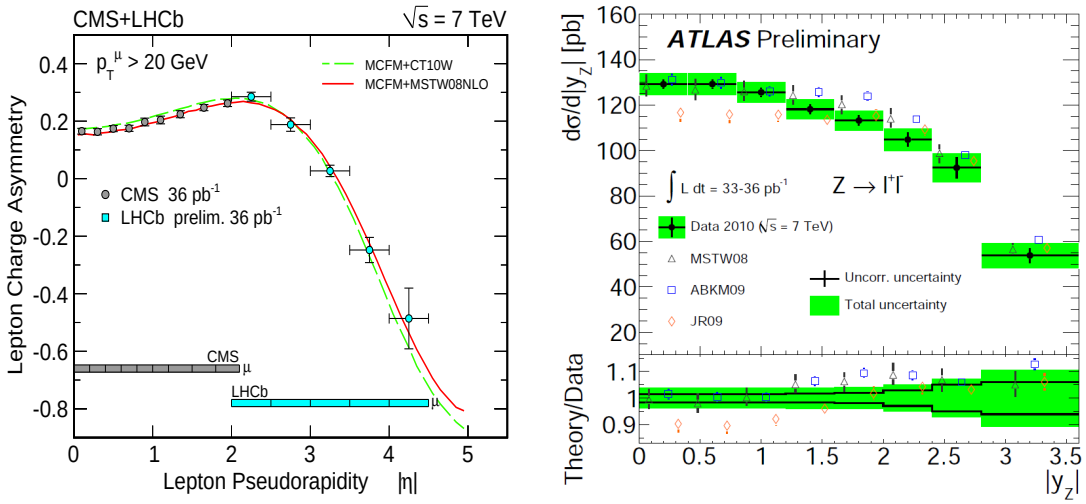

Figure 5: Left: W lepton charge asymmetry measurements of LHCb, compared with CMS measurements at lower pseudo-rapidities. Right: ATLAS measurements of the differential $Z \to \ell^+\ell^-$ cross section as a function of the Z rapidity, compared with theoretical predictions.

correspond to high-p_T lepton pairs accompanied by hard jets. Experimental results are in nice agreement with the predictions from FEWZ.

The ATLAS collaboration has started efforts to understand in detail the W and Z differential distributions as a function of the boson transverse momentum [19]. The understanding of these distributions at low boson momenta is an essential step in the path towards a precise measurement of the W mass at the LHC, whereas a precise understanding at high momenta could be important in the case of new physics effects related with associated weak boson production. Fig. 6-right shows the measurement for the W case, compared with different theoretical predictions. Observing a reasonable agreement between data and leading-order Monte Carlos like PYTHIA or ALPGEN is not surprising, given the fact that PYTHIA has been extensively tuned on previous data. Similarly, NLO approaches like POWHEG or MC@NLO show disagreements that may be due to the absence of specific NLO tunings at present. More surprising is the observed disagreement between data and RESBOS [20], a program that provides predictions at NNLO order and next-to-next to leading-log (NNLL) order at the level of gluon resummation, which should be precise enough in the fully perturbative region $p_T(W) \gtrsim 4$ GeV. More work is necessary to understand in depth the origin of these discrepancies.

4. Selected results on weak bosons plus heavy quark jets

First LHC results on W production in association with charm jets by the CMS collaboration are reported in [21]. The process is extremely sensitive to the strange quark content of the proton, an important source of systematic uncertainties for future precision studies, like the measurement of the W mass. Charm jets are identified via secondary vertex information, since the $W + b$ component is small and top backgrounds can be estimated with the help of data control

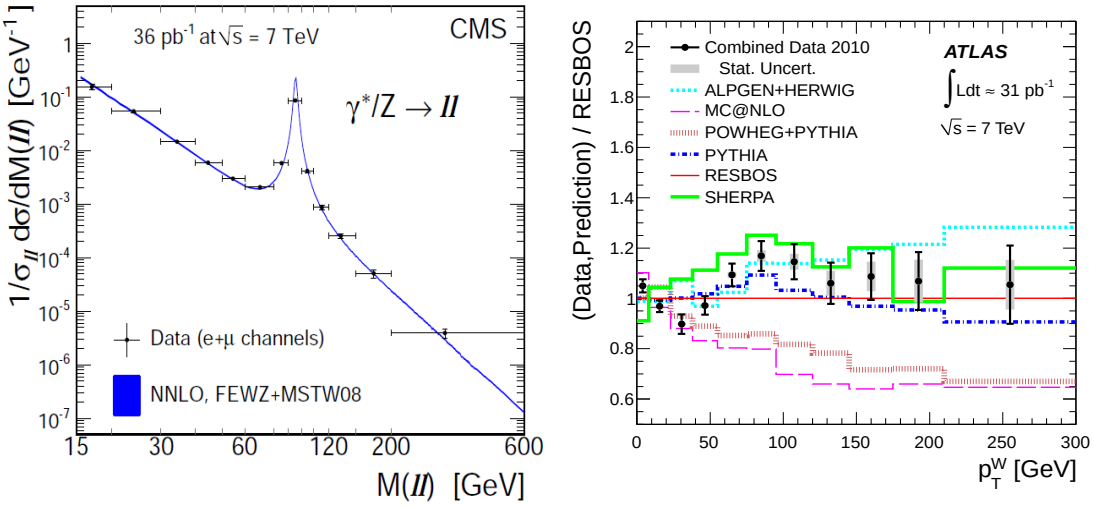

Figure 6: Left: CMS normalized dilepton differential cross section distribution as a function of the dilepton mass. Right: ATLAS W differential distribution as a function of the boson transverse momentum, compared with different theoretical predictions.

samples. Remaining light-quark backgrounds due to tracking resolution effects are efficiently constrained by fitting the number of vertices consistent with a negative decay length. Fig. 7-left shows the distribution of the secondary vertex discriminant variable for the W^+ case, after fitting of the dominant components in the sample. CMS obtains a preliminary value of the W+charm charge ratio: $\sigma(W^+ + c)/\sigma(W^- + c) = 0.92 \pm 0.19\ (stat.) \pm 0.04\ (syst.)$ and of the relative charm fraction: $\sigma(W + c)/\sigma(W + \geq 1\ \text{jet}) = 0.143 \pm 0.015\ (stat.) \pm 0.024\ (syst.)$, referred to jets with $p_T > 20$ GeV and $|\eta_{\text{jet}}| < 2.1$. Both measurements are in agreement with current PDF sets within statistical and systematic uncertainties.

CMS and ATLAS collaborations have already observed clear $Z+b+X$ signals in 2010 data [22], although with large uncertainties. More precise are the results from the CDF collaboration presented at this conference [23]: $\sigma(Z+b)/\sigma(Z+\text{jets}) = 0.0224 \pm 0.0024(stat.) \pm 0.0027\ (syst.)$, for an integrated luminosity of 7.8 fb^{-1}. This process is not only important as a test of perturbative QCD, but as a major background in many new physics searches (like Higgs searches below the WW mass threshold). The experimental results are in agreement with current theoretical estimates within uncertainties.

Another special process is $W+b+X$. Direct $parton + parton \rightarrow W + b$ production is largely CKM-suppressed, and therefore the signal is dominated by states produced via gluon-splitting ($W + g^* \rightarrow W + b\bar{b}$) and other higher order processes. Like in the $Z+b$ case, an understanding of this process is critical for many new physics searches, and there have been indications of an unexpected excess at CDF in the past [24]. The ATLAS collaboration has presented at this conference a first study of $W+b+X$ production with $\mathscr{L} = 35$ pb^{-1} [25]. The analysis is challenging, due to the presence of large backgrounds from $W+c$ and particularly from top production. The $W+c$ component is suppressed with very tight cuts on b-tagging, whereas top backgrounds require a dedicated set of veto cuts. The results are presented in Fig. 7-right. They point to a central value

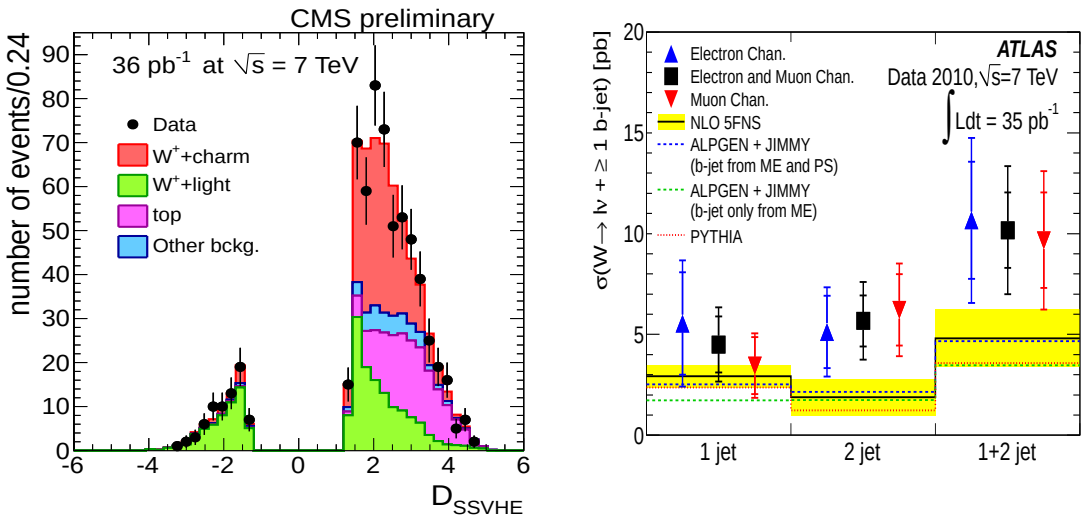

Figure 7: Left: secondary vertex discriminant distribution in the $W + charm + X$ analysis of the CMS collaboration (W^+ sample shown). Right: measurements of the $W + bottom + X$ cross section by the ATLAS collaboration as a function of the number of jets considered in the final state.

of the $W + b + X$ cross sections slightly higher than the one predicted by Monte Carlo, although present uncertainties are still large.

5. Diboson cross sections, anomalous triple gauge couplings

Triggered by Higgs boson searches with the maximum integrated luminosities collected until Summer 2011, Tevatron and LHC experiments have analyzed a substantial fraction of the available statistics and have measured WW, ZZ and WZ cross sections. Given the relevance of the new results, we will briefly describe the latest measurements by ATLAS and CMS, corresponding to $\mathscr{L} \approx 1$ fb^{-1}.

A rather clean sample of WW events at the LHC (≈ 400 events with $\approx 40\%$ background) is obtained by considering only fully leptonic W decays and by applying stringent criteria to reject the numerous background contributions: W plus jets, top backgrounds, Drell-Yan, $Z \to \tau^+\tau^-$, multi-jet events and other diboson final states. The electron and muon identification criteria are similar to the ones used in inclusive W analyses. Drell-Yan events are largely suppressed by vetoing dilepton candidates consistent with a Z decay and events with no significant $E_{\mathrm{T}}^{\mathrm{miss}}$. Events with taus are rejected by requiring that the direction of $E_{\mathrm{T}}^{\mathrm{miss}}$ is not consistent with one of the lepton directions. Top, W plus jets and multijet backgrounds are reduced by vetoing the presence of jets above some minimal transverse energy, $p_{\mathrm{T}} > 30$ GeV, whereas events with more than two leptons are not considered in order to suppress WZ and ZZ final states. Most backgrounds, and particularly the dominant ones after cuts - W plus jets, $t\bar{t}$ and Drell-Yan - are controlled via data-driven methods (e.g. using samples with relaxed lepton identification cuts, b-tagged control samples and same-sign dileptons). Fig. 8-left shows the distribution of the transverse momentum of the leading lepton after cuts measured by ATLAS, in good agreement with expectations. More details can be found in the Notes presented at this Conference [26, 27].

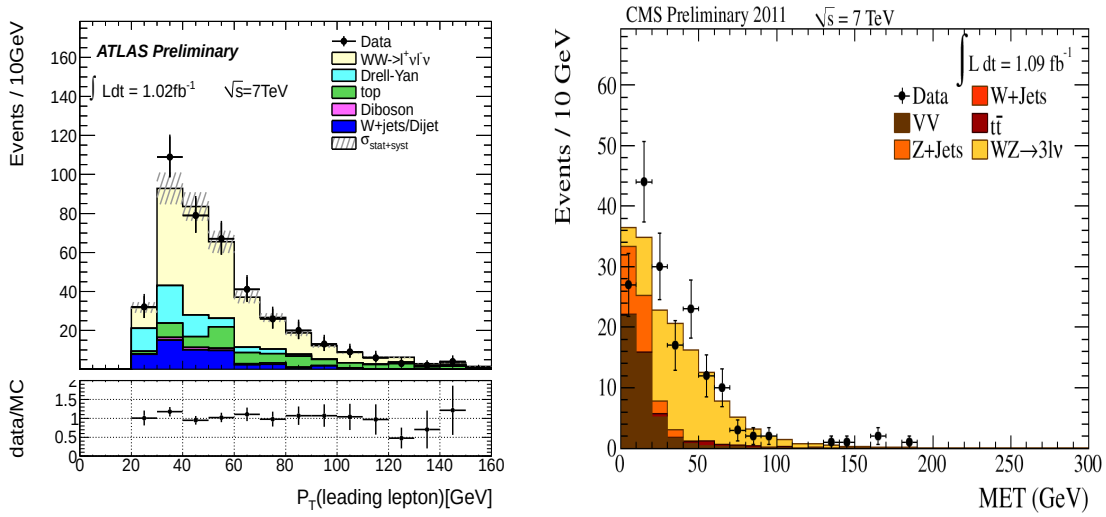

Figure 8: Left: Transverse momentum distribution of the leading lepton in ATLAS WW selected events. Right: $E_{\mathrm{T}}^{\mathrm{miss}}$ distribution of CMS WZ selected events.

The WZ channel is cleaner than WW. For $\mathscr{L} = 1$ fb^{-1} one has typical yields of $\approx 70-80$ events with $\approx 10-15\%$ background in the fully leptonic case. Analysis strategies are similar in ATLAS and CMS [28, 26]. Besides the selection of e^+e^- and $\mu^+\mu^-$ combinations consistent with the Z resonance, the signature demands the presence of a third muon or electron and significant $E_{\mathrm{T}}^{\mathrm{miss}}$. Like in the WW case, the critical backgrounds - Z plus jets and $t\bar{t}$ - are estimated using control samples in data whereas minor contaminations - ZZ, $Z\gamma$ - are estimated directly from Monte Carlo. Fig. 8-right shows the $E_{\mathrm{T}}^{\mathrm{miss}}$ distribution of selected events in data from CMS after final cuts, in agreement with Monte Carlo predictions.

ZZ is the cleanest channel, thanks to the availability of a double Z mass constraint. For $\mathscr{L} = 1$ fb^{-1} one has at the LHC typical yields of ≈ 10 events with almost negligible backgrounds [29, 26]. Lepton isolation criteria and transverse momentum cuts are slightly relaxed with respect to the Z inclusive analysis to gain some efficiency. The small remaining contaminations - $Zb\bar{b}$, $t\bar{t}$ - are nevertheless studied in data using background-enriched control samples. Fig. 9-left shows the distribution of the reconstructed invariant mass of the four-lepton system after cuts, as measured by CMS. The clean nature of the ZZ signature allows to even consider final states affected by larger backgrounds, like $ZZ \to \ell^+\ell^-\tau^+\tau^-$ (CMS [26]).

Diboson cross sections have recently been measured at Tevatron using large integrated luminosities, $\mathscr{L} \approx 6$ fb^{-1}, observing yields comparable to the LHC yields reported before. Fig. 9-right summarizes the remarkable achievements of Tevatron experiments over many years of data taking, from the measurement of single weak boson cross sections to the measurement of diboson cross sections at the picobarn level, not far from the threshold of observability of Higgs production [30]. All results are in excellent agreement with Standard Model expectations.

Diboson yields are directly sensitive to the triple gauge boson couplings predicted in the Standard model (W^+W^-Z, $W^+W^-\gamma$). New anomalous triple gauge boson couplings (aTGC) and deviations from the Standard Model predictions would lead to an enhancement of the measured cross

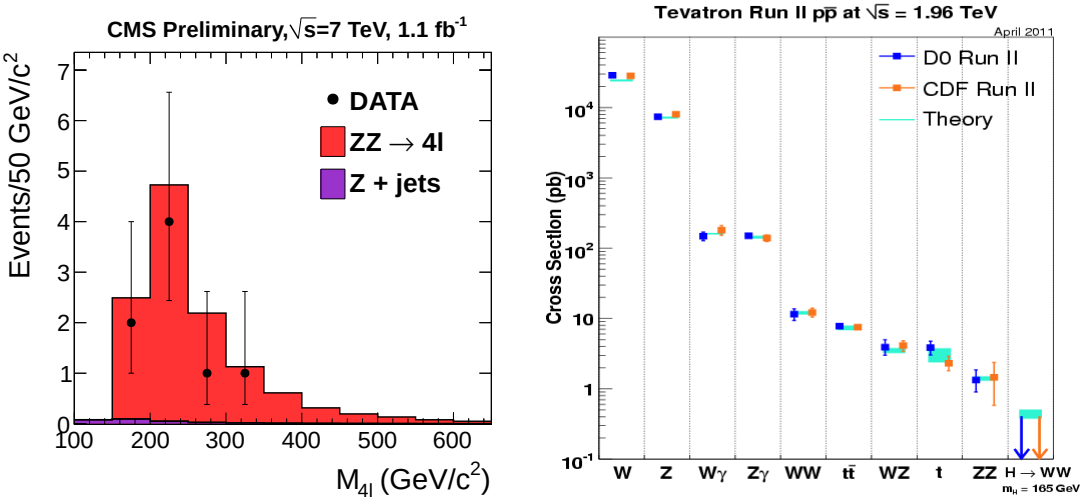

Figure 9: Left: Four-lepton invariant mass distribution for ZZ selected events (CMS). Right: summary of weak boson cross sections measured at Tevatron.

sections, particularly at large values of the diboson masses. These aTGC features place the LHC in an advantageous position with respect to Tevatron, thanks to the larger $\sqrt{s}$ of the hadron collisions. Fig. 10-left shows the example of the ATLAS ZZ analysis [29]. The study of ZZV anomalous couplings uses only the total ZZ measured cross section, but the obtained limits are more stringent than previous limits from LEP and Tevatron. In any case, Tevatron studies have at present similar or even better sensitivities in most cases, thanks to the use of kinematic information and more elaborated analyses. Fig. 10-right shows the example of W^+W^-Z aTGC studies in the WZ channel by the *D*0 collaboration [30], providing the most stringent limits on W^+W^+V anomalous couplings to date.

References

[1] T. Sjostrand, S. Mrenna, P. Skands, *PYTHIA 6.4 Physics and Manual*, JHEP 0605 (2006) 026 [hep-ph/0603175], G. Corcella *et al.*, *HERWIG 6.5: an event generator for Hadron Emission Reactions With Interfering Gluons (including supersymmetric processes)*, JHEP 0101:010,2001 [hep-ph/0011363].

[2] S. Frixione and B.R. Webber, *Matching NLO QCD computations and parton shower simulations* JHEP 0206 (2002) 029, [hep-ph/0204244], S. Frixione, P. Nason, C. Oleari, *Matching NLO QCD computations with parton shower simulations: the POWHEG method*, JHEP 0711 (2007) 070, [arXiv:0709.2092]

[3] K. Melnikov, F. Petriello, *Electroweak gauge boson production at hadron colliders through $O(\alpha_s^2)$*, Phys. Rev. D74 (2006) 114017, [hep-ph/0609070], S. Catani *et al.*, *Vector Boson Production at Hadron Colliders: A Fully Exclusive QCD Calculation at Next-to-Next-to-Leading Order*, Phys. Rev. Lett. 103 (2009) 082001, [arXiv:0903.2120].

[4] M.L. Mangano *et al.*, *ALPGEN, a generator for hard multiparton processes in hadronic collisions*, JHEP 0307 (2003) 001, [hep-ph/0206293], J. Alwall *et al.*, *MadGraph/MadEvent v4: the new web*

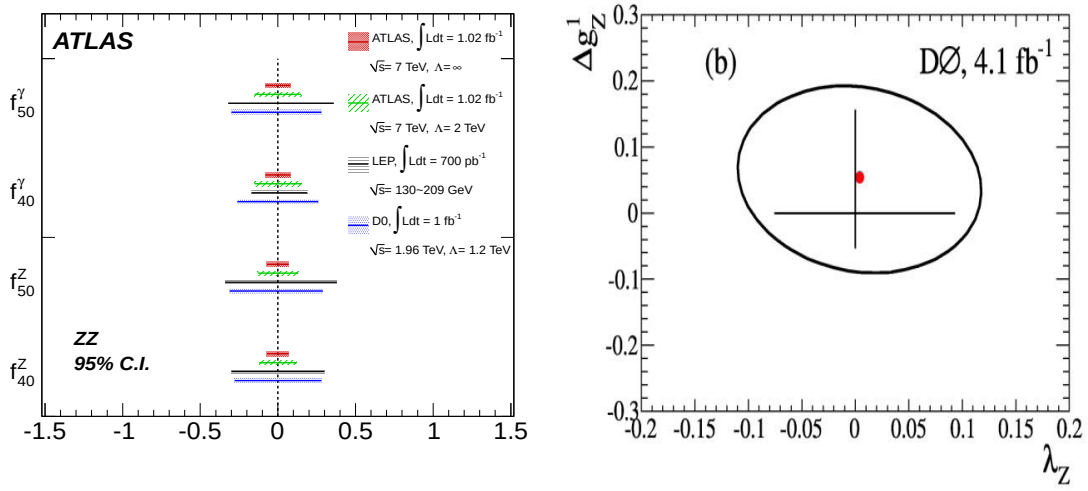

Figure 10: Left: *ZZV* anomalous triple gauge coupling limits from the ATLAS collaboration. Right: W^+W^-Z anomalous triple gauge coupling limits from the studies of WZ final states by the D0 collaboration.

generation, JHEP 0709 (2007) 028, [arXiv:0706.2334], T. Gleisberg *et al.*, *Event generation with SHERPA 1.1*, JHEP 0902 (2009) 007, [arXiv:0811.4622].

[5] J. Alwall *et al.*, *MadGraph 5 : Going Beyond*, JHEP 1106 (2011) 128, [arXiv:1106.0522], S. Hoeche *et al.*, *Next-to-leading order matrix elements and truncated showers*, [arXiv: 1009.1477].

[6] ATLAS Collaboration, *The ATLAS experiment at the CERN LHC*, JINST 3 (2008) S08003, CMS Collaboration, *The CMS experiment at the CERN LHC*, JINST 3 (2008) S08004, LHCb Collaboration, *The LHCb Detector at the LHC*, JINST 3 (2008) S08005.

[7] CDF Collaboration, *The CDF-II detector: Technical design report*, FERMILAB-PUB-96-390-E, D0 Collaboration, *The upgraded D0 Detector*, Nucl. Instrum. Meth. A565 (2006) 463.

[8] ATLAS Collaboration, *A measurement of the total* W^+ *and* $Z/$ *cross sections in the e and* μ *decay channels and of their ratios in pp collisions at* $\sqrt{s} = 7$ *TeV with the ATLAS detector*, ATLAS-CONF-2011-041.

[9] CMS Collaboration, *Measurement of the W and Z inclusive production cross sections at* $\sqrt{s} = 7$ *TeV with the CMS experiment at the LHC*, CMS-PAS-EWK-10-005.

[10] ATLAS Collaboration, *Measurement of the* $Z \to \tau^+\tau^-$ *Cross Section with the ATLAS Detector*, [arXiv:1108.2016].

[11] CMS Collaboration, *Measurement of the Inclusive Z Cross Section via Decays to Tau Pairs in pp Collisions at* $\sqrt{s} = 7$ *TeV*, J. High Energy Phys. 08 (2011) 117, [arXiv:1104.1617].

[12] LHCb Collaboration, *Updated measurements of W and Z production at* $\sqrt{s} = 7$ *TeV with the LHCb experiment*, LHCb-CONF-2011-039.

[13] CMS Collaboration, *Measurement of the lepton charge asymmetry in inclusive W production in pp collisions at* $\sqrt{s} = 7$ *TeV*, J. High Energy Phys. 04 (2011) 050, [arXiv:1103.3470].

[14] M. Bellomo, *W and Z production measured using the ATLAS detector, and impact on partons densities of the proton*, parallel presentation at this conference.

[15] NNPDF Collaboration, R.D. Ball *et al.*, *Reweighting and Unweighting of Parton Distributions and the LHC W lepton asymmetry data*, [arXiv:1108.1758].

[16] LPCC Electroweak Working Group, internal communication.

[17] CMS Collaboration, *Differential Cross Sections for Z Bosons at* $\sqrt{s} = 7$ *TeV*, CMS-PAS-EWK-10-010.

[18] CMS Collaboration, *Measurement of the Drell-Yan Cross Section in pp Collisions at* $\sqrt{s} = 7$ *TeV*, [arXiv:1108.0566].

[19] ATLAS Collaboration, *Measurement of the transverse momentum distribution of* $Z/^*$ *bosons in proton-proton collisions at* $\sqrt{s} = 7$ *TeV with the ATLAS detector*, [arXiv:1107.2381] and *Measurement of the Transverse Momentum Distribution of W Bosons in pp Collisions at* $\sqrt{s} = 7$ *TeV with the ATLAS Detector*, [arXiv:1108.6308].

[20] C. Balazs, C.P. Yuan, *Soft gluon effects on lepton pairs at hadron colliders*, Phys. Rev. D56 (1997) 5558, [hep-ph/9704258].

[21] CMS Collaboration, *Study of associated charm production in W final states at* $\sqrt{s} = 7$ *TeV*, CMS-PAS-EWK-11-013.

[22] CMS Collaboration, *Observation of Z+b*, CMS-PAS-EWK-10-015, ATLAS Collaboration, *Measurement of the cross-section for b-jets produced in association with a Z boson at* $\sqrt{s} = 7$ *TeV with the ATLAS detector*, [arXiv:1109.1403].

[23] CDF Collaboration, *Measurement of the b jet Production Cross Section for events with a Z boson with* 7.8 fb^{-1} *of data*, CDF note 10594.

[24] CDF Collaboration, *First Measurement of the b-Jet Cross Section in Events with a W Boson in* $p\bar{p}$ *Collisions at* $\sqrt{s} = 1.96$ *TeV*, [arXiv:0909.1505].

[25] ATLAS Collaboration, *Measurement of the cross section for the production of a W boson in association with b-jets in pp collisions at* $\sqrt{s} = 7$ *TeV with the ATLAS detector*, [arXiv:1109.1470].

[26] CMS Collaboration, *Measurement of the WW, WZ and ZZ cross sections at CMS*, CMS-PAS-EWK-11-010.

[27] ATLAS Collaboration, *Measurement of the* W^+W^- *production cross section in proton-proton collisions at* $\sqrt{s} = 7$ *TeV with the ATLAS detector* ATLAS-CONF-2011-110.

[28] ATLAS Collaboration, *Measurement of the* W^+Z *Production Cross-Section in Proton-Proton Collisions at* $\sqrt{s} = 7$ *TeV with the ATLAS Detector*, ATLAS-CONF-2011-099.

[29] ATLAS Collaboration, *Measurement of the ZZ production cross section and limits on anomalous neutral triple gauge couplings in proton-proton collisions at* $\sqrt{s} = 7$ *TeV with the ATLAS detector*, [arXiv:1110.5016].

[30] U. Bassler, *Di-boson physics at D0*, parallel presentation at this Conference.